JTTEE5 9:204-209
© ASM International

Peer Reviewed

Effect of Heat Treatment on the Thermal Conductivity of Plasma-Sprayed Thermal Barrier Coatings

Rollie Dutton, Robert Wheeler, K.S. Ravichandran, and K. An

(Submitted 30 December 1998; in revised form 5 December 1999)

The effect of heat treatment on the thermal conductivity of plasma-sprayed Y_2O_3 stabilized ZrO_2 (YSZ) and Al_2O_3 coatings was investigated. A heat treatment of 1300 °C in flowing argon for 50 h was found to significantly increase the thermal conductivity of the coatings when compared to measurements in the as-sprayed condition. Transmission electron microscopy (TEM) examination of the microstructures of the coatings in the as-sprayed and heat-treated conditions revealed that sintering of microcracks at the splat interfaces was the main cause for the increase in thermal conductivity. In the YSZ coatings, complete closure of microcracks was frequently observed. In contrast, microcrack closure in the Al_2O_3 coatings was characterized by the isolated necking of particles across a microcrack rather than complete closure. A model for thermal conductivity in a solid containing oriented penny-shaped cracks was used to explain the observed increase in thermal conductivity after heat treatment.

Keywords thermal conductivity, heat treatment, microcracks, TBCs

1. Introduction

The thermal conductivity of plasma-sprayed thermal barrier coatings (TBCs) is strongly dependent upon the porosity of the coating and the thermal resistance at the splat interfaces.[1] These factors determine the heat insulation, thermal shock resistance, thermal cycle tolerance, and erosion resistance of the TBC. Since plasma spraying involves processing temperatures on the order of 6000 to 12,000 °C, one would expect the coating properties to be stable at operating conditions of 900 to 1100 °C. However, an increase in the thermal conductivity of TBCs with thermal exposure has often been observed.[2,3,4] Since TBCs are exposed to high temperatures for extended periods of time, an understanding of the change in thermal conductivity with thermal exposure is important. The purpose of this work is to elucidate the mechanisms governing this increase in thermal conductivity with thermal exposure.

2. Experimental Procedure

Plasma-sprayed coatings were obtained by spraying Y_2O_3 stabilized ZrO_2 (YSZ) and Al_2O_3 powder onto 3 mm thick René 95 substrates (62.5 × 12.5 mm). The YSZ powder (Metco 204NS, Sulzer Metco, Hicksville, NY) had an average particle size of 10 μm and a composition in wt.% of 8 Y_2O_3, 1.6 HfO_2, 0.1 TiO_2, 0.1 TaO, and 0.05 of combined CaO, Al_2O_3, Fe_2O_3, and MgO. The Al_2O_3 powder (Plasmalloy Al-1010, Sulzer Metco, Hicksville, NY) had an average particle size of 5 μm and a composition in wt.% of 0.3 Na_2O, 0.05 Fe_2O_3, and 0.02 SiO_2. The coatings were applied using a Plasma Technik Spray system with a single spray nozzle located at the Thermal Spray Laboratory of the State University of New York, (Stony Brook, NY). Calibration sprays were performed to control the layer thickness. Deposition was carried out for a specified time determined from the calibration runs for the required coating thickness. Samples measuring 10 × 10 mm were cut from the as-sprayed samples and heat treated for 50 h at 1300 °C under flowing argon (99.99% purity). The coatings separated from the substrate during the heat treatment and some reaction product adhered to the coating/substrate interface. This was removed by polishing prior to the determination of the thermal conductivity. To obtain a sample of the bulk YSZ material for reference thermal conductivity measurements, the as-received YSZ powder was hot pressed at 1500 °C for 1 h at 18 MPa. The hot-pressing cycle was designed such that the porosity of the hot-pressed sample was approximately the same as that of the as-sprayed YSZ coating. To allow a direct comparison between the thermal conductivity of the hot-pressed YSZ powder and the *as-sprayed* YSZ coating, the influence of the coating/substrate interface upon thermal conductivity was eliminated by chemically removing a sample of the YSZ coating from the superalloy substrate. The detached coating was polished prior to the determination of thermal conductivity.

The thermal conductivity was determined using the laser flash technique at the Thermophysical Properties Research Laboratory at Purdue University (West Lafayette, IN). The laser flash technique involves heating one side of the sample with a laser pulse of short duration and measuring the temperature rise on the other side with an infrared detector. The thermal diffusivity is determined from the time required to reach one-half of the peak temperature and a transient heat conduction analysis of a multilayer body. Measurements were made in a vacuum cham-

Rollie Dutton, Air Force Research Laboratory, AFRL/MLLM, Materials and Manufacturing Directorate, Wright-Patterson AFB, OH 45433-7817; **Robert Wheeler,** UES, Inc., Dayton, OH 45432; and **K.S. Ravichandran** and **K. An,** Department of Metallurgical Engineering, The University of Utah, Salt Lake City, UT 84112.

ber from room temperature to 1000 °C in 100 °C increments.[1] Specific heat measurements of the Al_2O_3 and YSZ powders were made with a Perkin-Elmer Model DSC-2 (PE Corp., Norwalk, CT) differential scanning calorimeter using sapphire as the reference material. The thermal conductivity of the coatings was then determined using

$$k = \alpha C_p \rho \quad \text{(Eq 1)}$$

where k is the thermal conductivity, α is the thermal diffusivity, C_p is the specific heat, and ρ is the density of the coating.

The porosity of the coatings was determined by measurement of coating mass and volume as well as by point counting using optical micrographs of the polished cross section at a magnification of 400×. The two techniques gave reasonable agreement. Examination of the as-sprayed and heat-treated samples indicated that the pores had dimensions on the order of microns, while the thin cracks at splat interfaces had separations on the order of nanometers. Hence, the pores, but not the microcracks, could be observed optically. While the microcracks could be observed using low voltage scanning electron microscopy, only transmission electron microscopy (TEM) provided the additional structural information to allow the microcracks to be related to the fine-grained regions of the splat interfaces. The microstructures of the coatings were studied by TEM using a Philips CM200 microscope operating at 200 kV (Philips Electronic Instruments Corp., Mahwah, NJ). Cross-sectional specimens were prepared of both as-sprayed and heat-treated coatings. In this manner, the built up structure of the TBC could be studied by observing each layer of the deposited oxide powder particles. This required mounting two coatings together in a back-to-back configuration using a hard epoxy. The glued assemblage was then sectioned and ground in a conventional fashion to produce a 3 mm disc having a dimple at the TBC layer. Finally, this disc was ion milled at a low angle (40° inclination) in a Gatan PIPS (Gatan, Pleasanton, CA) unit.

3. Results and Discussion

3.1 Porosity and Texture Measurements

The average porosity of the as-sprayed YSZ coating was found to be 11.9% ± 0.5% and the Al_2O_3 coating was 18.8% ± 1.5%. The average porosity of the hot-pressed YSZ powder was 12.5% ± 0.5%. Measurements after heat treatment indicated that any changes in the porosity level were on the order of statistical variations in porosity due to location within a given coating, *i.e.*, there was essentially no change in the porosity after heat treatment.

The X-ray diffraction pattern of the as-sprayed YSZ coating indicated that it consisted almost entirely of the tetragonal phase of ZrO_2. Similar results were found for the as-received and hot-pressed YSZ powder. It should be noted that the tetragonal phase in the as-sprayed YSZ coatings consists of a nontransformable tetragonal phase, known as the t' phase. This nonequilibrium phase is present because of the rapid cooling from the vapor to the bulk state upon deposition onto the substrate. The as-sprayed Al_2O_3 coating was a mixture of α and γ phases, while the Al_2O_3 powder contained only the α phase. Apparently, some of the high-temperature γ phase of Al_2O_3 was retained due to the rapid cooling of the splats during solidification. Heat treatment at 1300 °C for 50 h did not significantly alter the X-ray diffraction patterns of either coating, indicating that the phases present in the as-sprayed coatings are stable at the heat treatment temperature.

3.2 Thermal Conductivity Measurements

Figure 1(a) and (b) present the thermal conductivity measurements for the as-sprayed coatings and the fully dense coating material. The values of thermal conductivity shown for the bulk YSZ are for the tetragonal phase,[5] while those for the Al_2O_2 are for the α phase since values for the thermal conductivity of high-temperature γ phase are not available.[6] It is readily apparent that the thermal conductivity of the as-sprayed coatings is well below that of the bulk material. The effect of the heat treatment on the thermal conductivity is greatest at lower

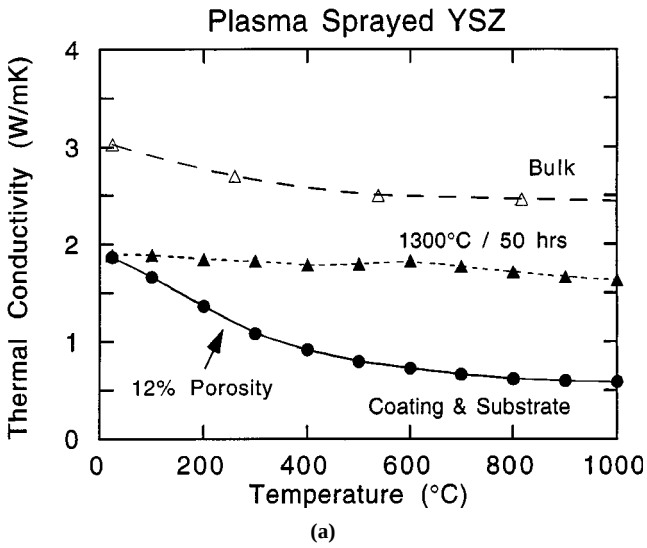

(a)

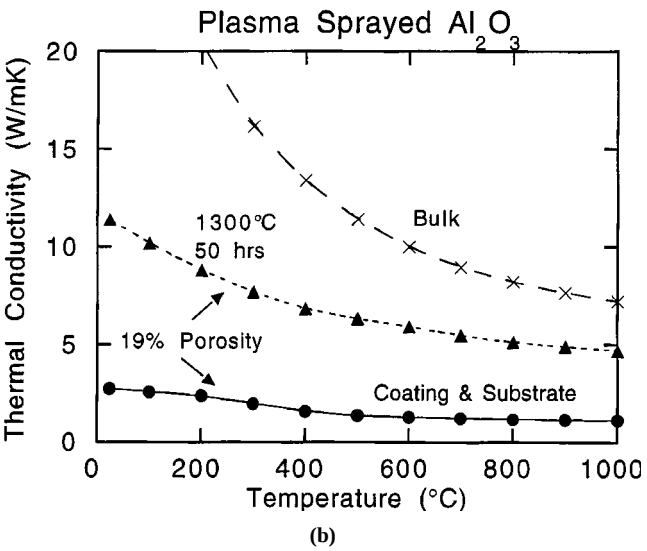

(b)

Fig. 1 (a) and (b) The thermal conductivity of plasma-sprayed YSZ and Al_2O_3 coatings in the as-sprayed and heat-treated conditions. The values of thermal conductivity for the bulk YSZ and Al_2O_3 are from Ref 5 and 6, respectively.

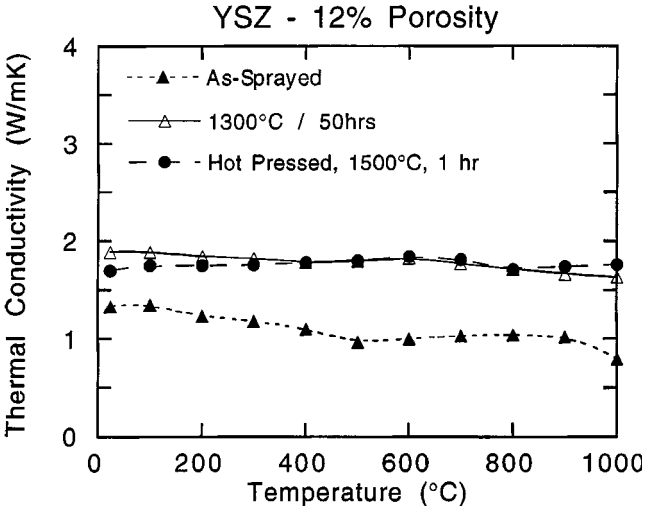

Fig. 2 The thermal conductivity of plasma-sprayed YSZ coatings in the as-sprayed and heat-treated conditions and hot-pressed YSZ powder. All samples have approximately 12% porosity. The plasma-sprayed coatings were detached from their substrates.

temperatures and decreases as the temperature increases. Selecting 1000 °C as a representative operating temperature for the coatings, it can be seen that after the heat treatment at 1300 °C for 50 h, there is a threefold increase in the thermal conductivity of the YSZ and a fivefold increase in the Al_2O_3. Figure 2 is a plot of the thermal conductivity for an as-sprayed YSZ coating that has been chemically removed from the substrate, a heat-treated plasma-sprayed coating, again detached from the substrate, and the hot-pressed YSZ powder. The YSZ coating was chemically removed to eliminate the effect of the coating/substrate interface upon the thermal conductivity measurements. (Similar attempts to chemically remove the Al_2O_3 coating were unsuccessful—during the etching of the substrate, the coating fragmented into small pieces.) The porosity of all three specimens is approximately 12%. It can be seen that the thermal conductivity of the heat-treated coating is essentially identical to that of the hot-pressed powder for all temperatures. Thus, the thermal conductivity measurements indicate that the heat treatment has eliminated any reduction in thermal conductivity due to the rapid solidification microstructure of plasma spraying.

3.3 Metallographic Observations

Figure 3 is a micrograph of the hot-pressed YSZ powder. The microstructure is characterized by uniform coarse grains (recall that the average powder size was 10 μm) and widely distributed pores. No microcracks were present within the sample. Figure 4(a) and (b) show examples of the as-sprayed microstructure for the YSZ coating. At low magnification (Fig. 4a), coarse grains are visible as well as pores and large microcracks. Some of the coarse grains are bound by layers exhibiting the fine-grained rapid solidification microstructure characteristic of plasma-sprayed coatings. At higher magnification (Fig. 4b), narrow micro cracks at the splat boundaries are apparent. In addition, some areas appear to have been subjected to remelting during the spraying process. The fact that no cracks were observed in the hot-pressed powder indicates that the observed microcracks are not

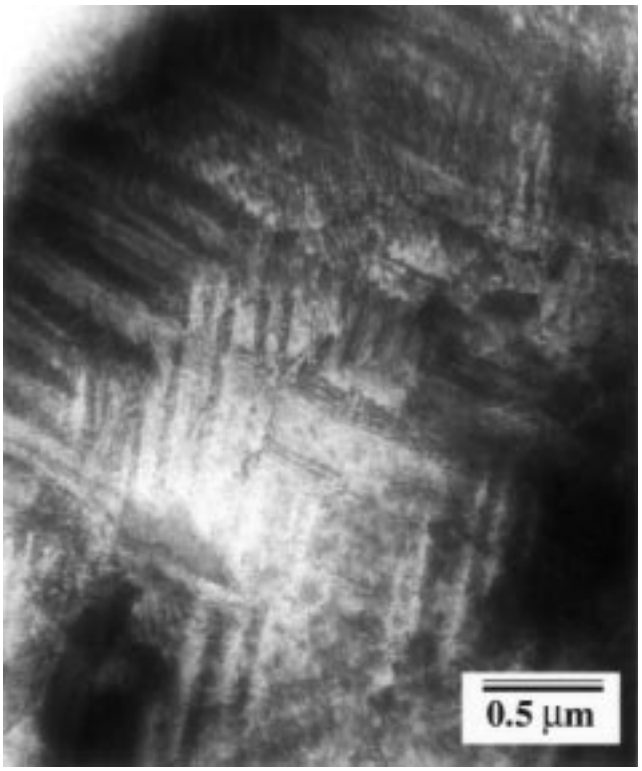

Fig. 3 TEM micrograph of hot-pressed YSZ powder

an artifact of the ion milling process. Hence, while both the hot-pressed powder and the as-sprayed coating contain pores, the plasma-sprayed coating contains areas of finer grains and a large population of micro cracks at the splat boundaries. Figure 5(a) and (b) are micrographs of the heat-treated coating. In Fig. 4(a) and (b), the wide cracks follow rather tortuous paths, while the narrower microcracks at splat interfaces are relatively straight or gently curving. These same trends are observed in Fig. 5(a) and (b), where the wide angular cracks remain open but extensive bridging occurs in the relatively straight cracks. Since both samples were ion milled at the same time, the closure of the microcracks can be attributed to the heat treatment. This suggests that areas with pores and wide microcracks (Fig. 5a) remained essentially unchanged after the thermal exposure, while narrow microcracks along the splat interfaces sintered closed.

Figure 6 show a typical microstructure for the as-sprayed Al_2O_3 coating. The coating contained coarse grains (recall that the powder size was 5 μm), pores, and microcracks along the splat boundaries. Figure 7(a) and (b) show typical heat treated microstructures. In contrast to the YSZ coating, the microcracks did not sinter closed. The grains along the microcrack boundaries became rounded (Fig. 7a) and formed necks intermittently across the microcrack (Fig. 7b), but for the most part, the microcracks remained open.

4. Discussion

While it is reasonable to expect that the sintering of the microcracks accounts for the threefold increase in thermal conductivity

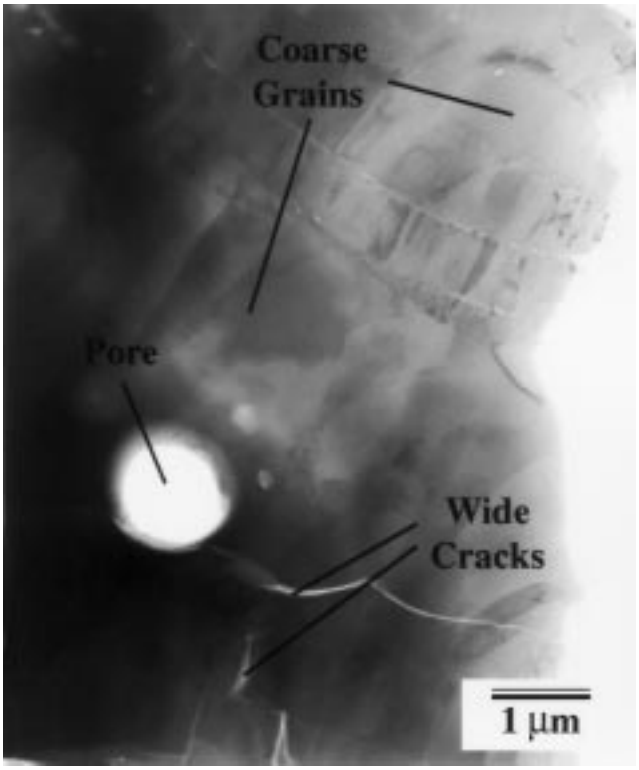

(a)

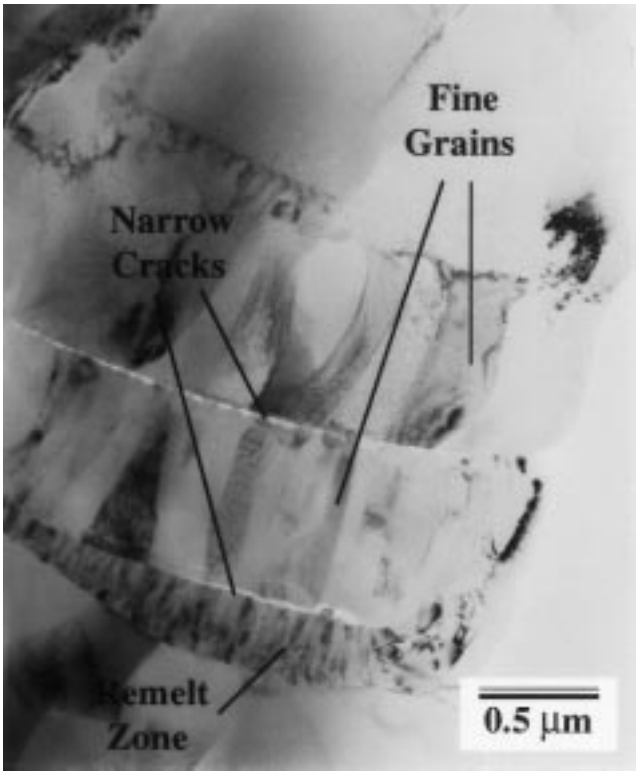

(b)

Fig. 4 (a) and (b) TEM micrographs of as-sprayed YSZ coating

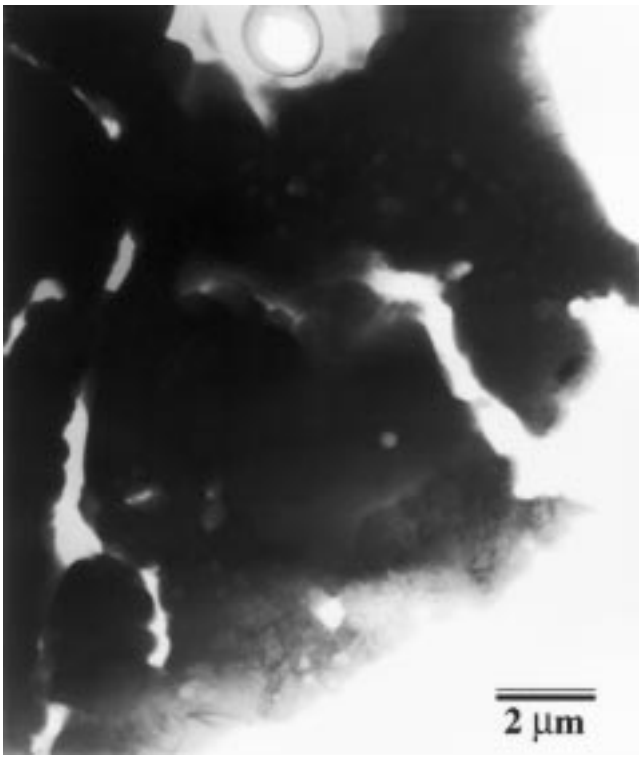

(a)

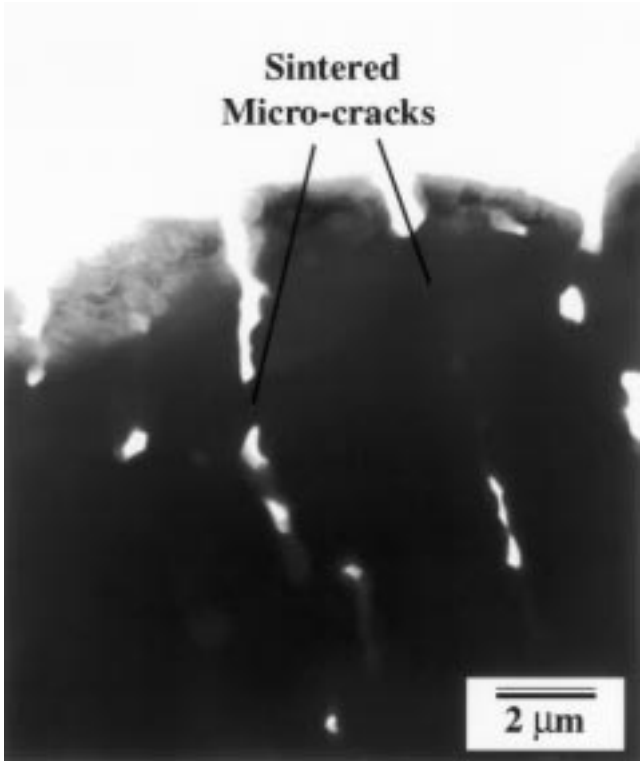

(b)

Fig. 5 TEM micrographs of YSZ coating following a heat treatment of 1300 °C for 50 h in flowing argon

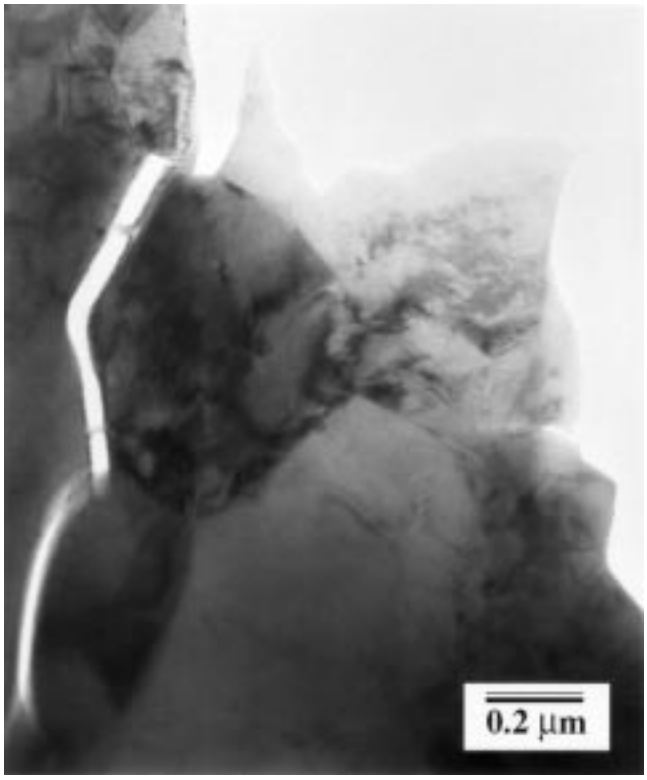

Fig. 6 TEM micrograph of as-sprayed Al_2O_3 coating

observed at 1000 °C in the heat-treated YSZ coating, it is not apparent that intermittent particle necking along microcrack boundaries can account for the fivefold increase in thermal conductivity observed in the Al_2O_3 coating. Hasselman[7] developed a model for the thermal conductivity of a material containing oriented penny-shaped cracks. His analysis assumed that the cracks were pores with a very flat shape equivalent to ellipsoids of revolution with the minor axis, approaching zero. For a dilute dispersion of penny-shaped cracks with zero thermal conductivity (*i.e.*, neglecting radiation and convection) and heat flow parallel to the minor axis of the crack, the relative thermal conductivity is

$$k/k_0 = \left(1 + (2V/\pi)(b/a)\right)^{-1} \quad \text{(Eq 2)}$$

where k is the thermal conductivity of the microcracked material, k_0 is the thermal conductivity of the uncracked material, V is the volume fraction of ellipsoidal pores, b is the major axis of the ellipsoid, and a is the minor axis. Figure 8 shows the model results for ellipsoids (*i.e.*, microcracks) with aspect ratios ranging from 20 to 500. Also shown is a best-fit line for the relative thermal conductivity of porous YSZ and Al_2O_3[1] using literature values. The relative thermal conductivity of the porous YSZ and Al_2O_3 is approximately linear with respect to the volume fraction of pores. In contrast, Hasselman's model predicts a sharp decrease in the relative thermal conductivity for the microcracked material for a relatively small volume fraction of ellip-

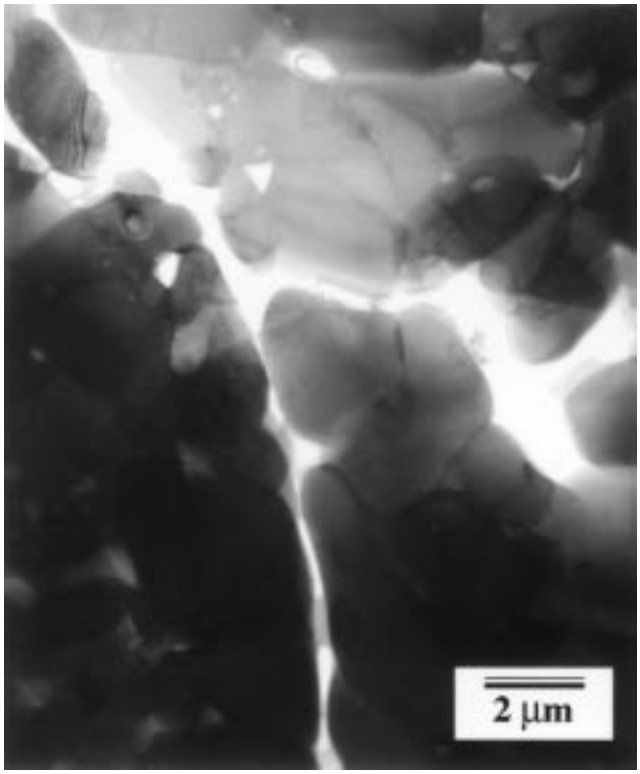

(a)

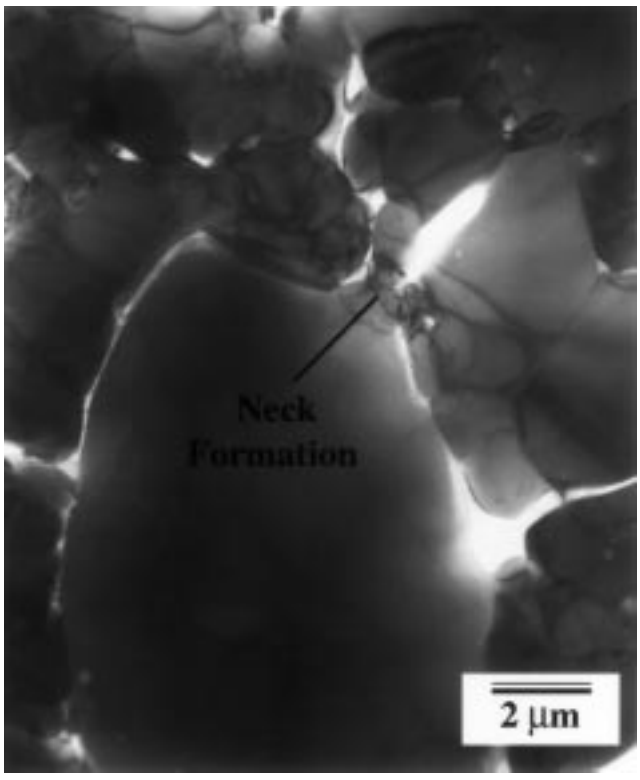

(b)

Fig. 7 (a) and (b) TEM micrographs of Al_2O_3 coating following a heat treatment of 1300 °C for 50 h in flowing argon

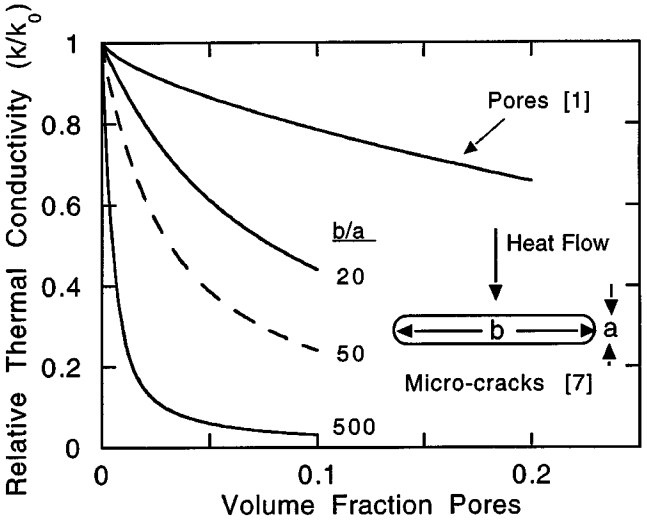

Fig. 8 Relative thermal conductivity for a material containing oriented penny-shaped microcracks with varying aspect ratios. Heat flow is parallel to the short axis of the microcrack. Also shown is a best-fit line for the experimental values of relative thermal conductivity for porous YSZ and Al_2O_3.

soidal pores (*i.e.*, $V < 0.05$). The severity of the drop increases as the aspect ratio of the microcracks increases. These predictions are similar to experimental results reported by Kingery *et. al.*[8] MgO-$MgAl_2O_3$ and Al_2O_3-ZrO_2 two-phase systems in which grain boundary microcracks occur.

Figure 4(a) and (b) Fig. 6 indicate that while the volume fraction of microcracks is small (*e.g.*, < 1%), their aspect ratio is very large (*e.g.*, >500). Figure 8 indicates that for this pore volume fraction and aspect ratio, the relative thermal conductivity is 0.24. Hence, if the microcracks sinter closed, there would be a fourfold increase in the thermal conductivity. Similarly, if the volume fraction of microcracks remained constant, but their aspect ratio changed from 500 to 20, there would be a fourfold increase in the thermal conductivity. This suggests that the increase in thermal conductivity after heat treatment can be explained by the changes in the microcracks at the splat boundaries. In the case of the YSZ, the microcracks sinter closed, while for the Al_2O_3, the aspect ratio of the cracks is reduced due to particle necking across the microcrack boundaries.

4. Summary and Conclusions

The effect of heat treatment on the thermal conductivity of plasma-sprayed YSZ and Al_2O_3 TBCs was investigated. A heat treatment of 1300 °C in flowing argon for 50 h was found to significantly increase the thermal conductivity of the coatings when compared to measurements in the as-sprayed condition. Examination of the microstructures of the coatings in the as-sprayed and heat-treated conditions revealed that sintering of microcracks at the splat interfaces was the main cause for the increase in thermal conductivity. In the YSZ coatings, complete closure of micro cracks was frequently observed. In contrast, microcrack closure in the Al_2O_3 coatings was characterized by the isolated necking of particles across a microcrack rather than complete closure.

Acknowledgments

The authors gratefully acknowledge the efforts of Dr. Ray Taylor for the thermal conductivity measurements and Scott Apt for the TEM foil preparation. Dr. Michael Maloney, Pratt & Whitney, and Dr. William Allen, United Technologies Research Center, generously shared results from their in-house work on the effect of pore shape on thermal conductivity. The work at the University of Utah was supported by U.S. Air Force Contract No. F33615-92-C-5900, through UES, Inc. (Dayton, OH).

References

1. K.S. Ravichandran, K. An, R.E. Dutton, and S.L. Semiatin: *J. Am. Ceram. Soc.*, 1999, vol. 82, pp. 673-82.
2. R.E. Taylor: *Mater. Sci. Eng.*, 1998, A245, vol. pp. 160-67.
3. L. Pawlowski and P. Fauchais: *Int. Metall. Rev.*, 1992, vol. 31, pp. 271-89.
4. L. Pawlowski, D. Lombard, and P. Fauchais: *J. Vac. Sci. Technol.* 1995, vol. 3, pp. 2494-2500.
5. D.P.H. Hasselman, L.F. Johnson, L.D. Bentsen, R. Syed, H.L. Lee, and M. v. Swain: *Am. Ceram. Soc. Bull*, 1987, vol. 66(5), pp. 799-806.
6. R.G. Munro: *J. Am. Ceram. Soc.*, 1997, vol. 80, pp. 1919-28.
7. D.P.H. Hasselman: *J. Comp. Mater.* 1978, vol. 12 (10), pp. 403-07.
8. W.D. Kingery, H.K. Bowen, and DR. Uhlmann: *Introduction to Ceramics*, Wiley-Interscience, New York, NY, 1976, pp. 640-42.